

TOUGHENING MECHANISMS IN MOLLUSK SHELLS

Roberto Ballarini
Case Western Reserve University
Cleveland, Ohio 44106-7201
roberto.ballarini@case.edu

Natural composite materials are renowned for their mechanical strength and toughness; despite being highly mineralized, with the organic component constituting not more than a few percent of the composite material, the fracture toughness exceeds that of single crystals of the pure mineral by two to three orders of magnitude. The judicious placement of the organic matrix, relative to the mineral phase, and the hierarchical structural architecture extending over several distinct length scales both play crucial roles in the mechanical response of natural composites to external loads. In this talk experimental and theoretical results are used to show that the resistance of the shell of the conch *Strombus gigas* to catastrophic fracture can be understood quantitatively by invoking two energy-dissipating mechanisms: multiple cracking in the outer layers at low mechanical loads, and crack bridging in the shell's tougher middle layers at higher loads. Both mechanisms are intimately associated with the so-called crossed lamellar microarchitecture of the shell, which provides for tunnel cracking in the outer layers and uncracked structural features that bridge crack surfaces, thereby significantly increasing the work of fracture, and hence the toughness, of the material. Despite a high mineral content of about 99% (by volume) of aragonite, the shell of *Strombus Gigas* can thus be considered 'ceramic plywood' (albeit plywood fails in a different manner than the shell), and can guide the bioinspired design of tough, lightweight structures.

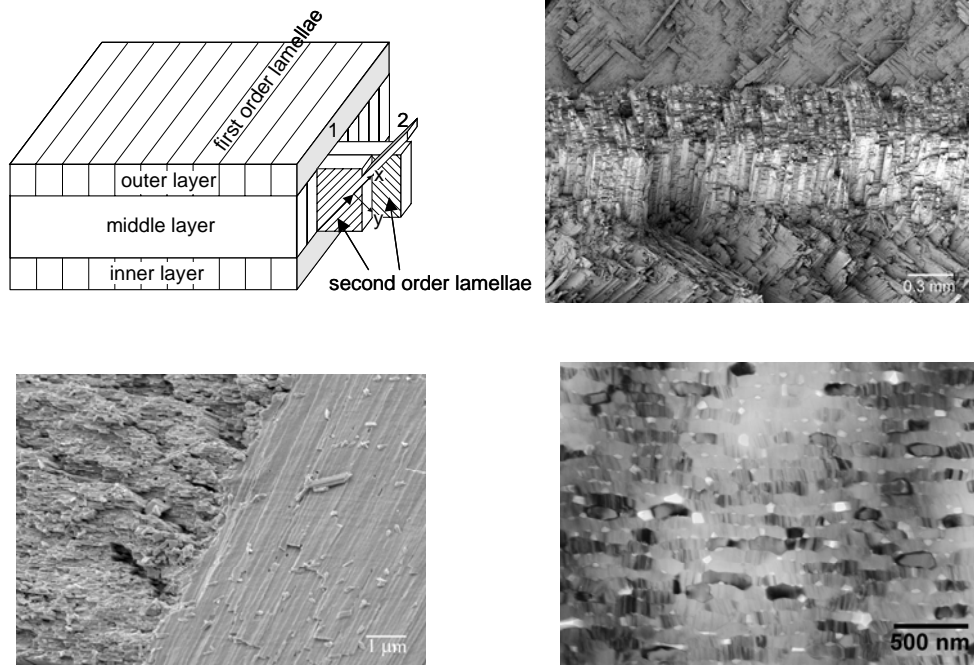


Figure 1 (upper-left) Schematic drawing of the microstructure of the conch shell. The bulk of the shell in mature animals contain 3 layers, as depicted here. Each layer contains first order, second order and third order lamellae. The twinned third order lamellae are not shown in this drawing, which emphasizes the $\pm 90^\circ$ orientation of second order lamellae within adjacent first order lamellae. (Second order lamellae are only shown for two first order lamellae in the middle layer.) The twinned third order lamellae are the basic building blocks of the structure. The first order interfaces are weak and favor multiple microcracking in the inner and outer (weak) layers, whereas 2nd-order interfaces favor crack deflection in the middle (tough) layer, as indicated by the bold arrow. The layers are 0.5 to 2 mm thick; the first order lamellae are 5-60 μm thick and many μm wide; the second order lamellae 5-30 μm thick and 5-60 μm wide; and the third order lamellae 60-130 nm thick and 100 nm wide. All third order lamellae are surrounded by sheaths of protein; similar proteinaceous material some 10 to 320 nm in thickness comprise the interfaces separating second order and first order lamellae, as well as the layer interfaces; (upper-right) and (lower-left) are SEM micrographs; the layer structure is easily discerned by the roughness resulting from cracks propagating parallel or perpendicular to first order lamellar interphases in the middle layer. The rough/smooth transition in adjacent first order lamellae is shown at high magnification in (lower-left); finally, (lower-right) is a TEM micrograph of a second order lamella taken in an “end-on” orientation. Individual twinned third order lamellae are revealed by diffraction contrast; the striped vertical features are twin boundaries. Although not apparent in this image, each third order lamella is encased in a proteinaceous sheath; globular protein is also present.

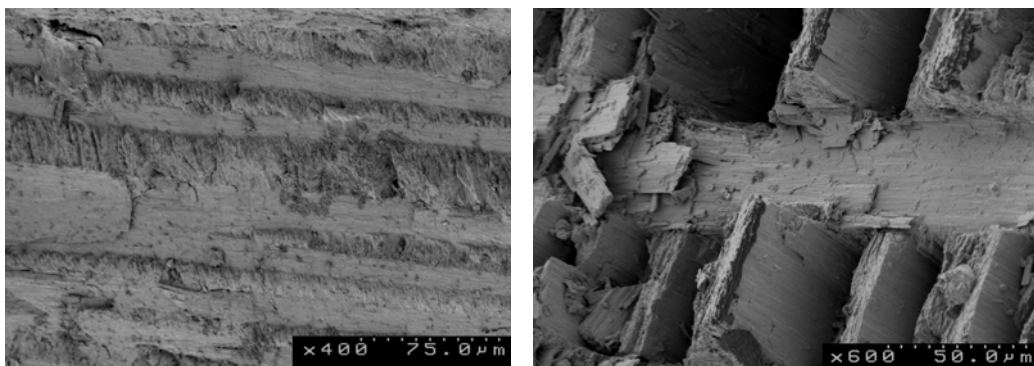


Figure 2 Fracture surfaces comprised of alternating smooth and rough regions at (a) -120°C and (b) 200°C .

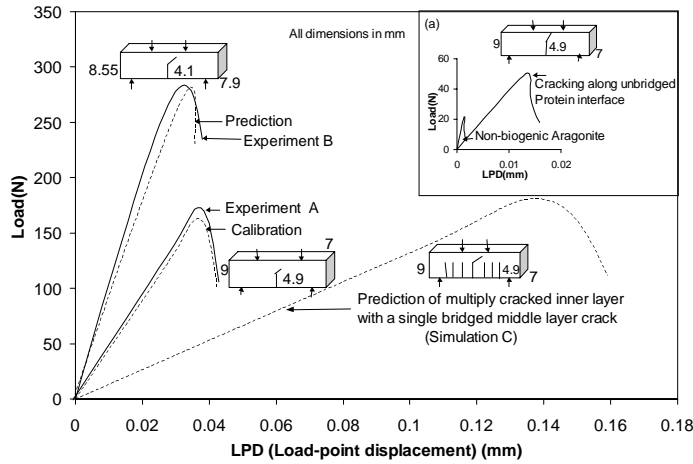


Figure 3 Experimental and theoretical load-deflection curves for specimens containing middle layer notches from Experiment A and Experiment B (two different geometries to validate the parameters). The theoretical unnotched beam response (simulation C, involving multiple cracking followed by a single tunnel crack propagating through the bridged middle layer) can be compared with the theoretically predicted response (see inset) of a beam comprised solely of non-biogenic aragonite ($K_C = 0.25 \text{ MPa}\cdot\text{m}^{1/2}$) or a beam in which cracks propagate unbridged along a mineral-protein interface ($K_C = 0.6 \text{ MPa}\cdot\text{m}^{1/2}$).

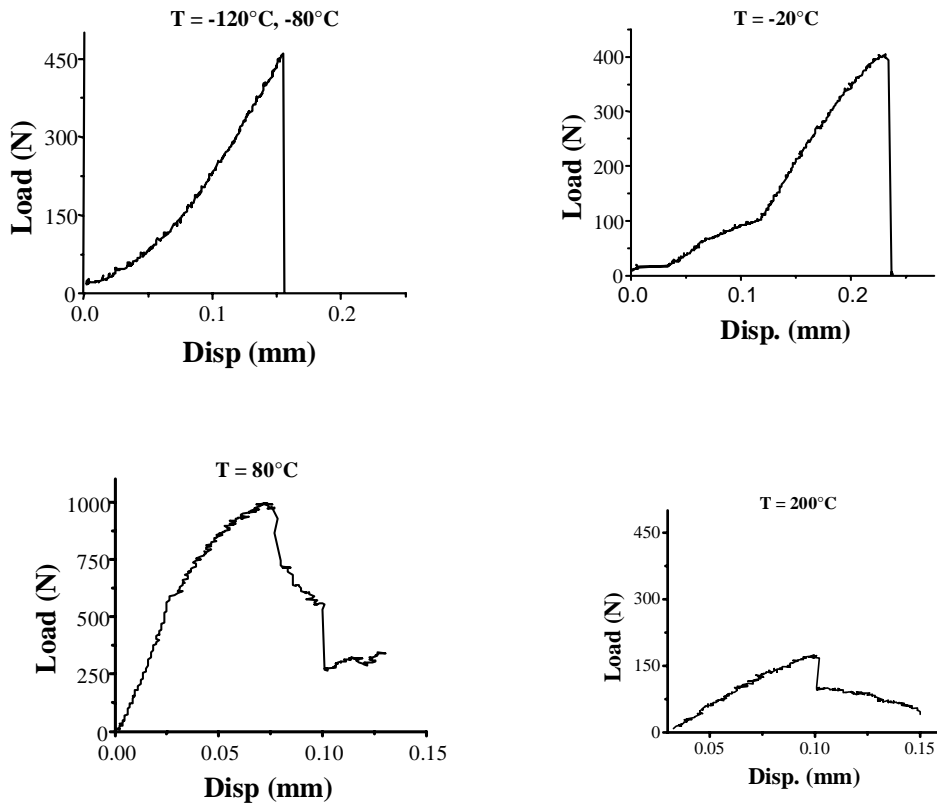


Figure 4 Load deflection curve of dry unnotched sample. At low temperatures (A and B), the sample did not show any post peak behavior and the fracture behavior is very “brittle”. As the temperature increases, the bridging becomes more efficient. At high temperatures (D), the samples did not show much load-bearing capabilities.